Journal of Materials, Processes and Environment
May edition. Vol. 5. N° 1. (2017)
ISSN : 2335-1020

Eugenia Caryophyllata extract as green inhibitor for steel corrosion in 1 M HCl solution

L. Allam[1], C. OULMAS[1], D. Boughrara[1], A. KADRI[1], N. BENBRAHIM[1]

[1.] Laboratory of Physical and Chemistry of Materials (LPCM) University of Tizi-Ouzou, BP 17 RP 15000, ALGERIA

ABSTRACT — The aim of this article is to study the Eugenia Caryophyllata extract (ECE) like a green corrosion inhibitor of steel in 1 M hydrochloric acid solution (HCl). The extract was obtained by hydro-distillation and then it was characterized by gas chromatography coupled with mass spectroscopy (GC/MS). Its efficiency was evaluated by electrochemical measurements (linear polarization resistance (LPR) potentiodynamic polarization (PP) and electrochemical impedance spectroscopy (EIS)) and non electrochemical methods like gravimetry and surface observations by scanning electron microscope (SEM). The results revealed that the extract behaves as an effective mixed inhibitor, and that the inhibition efficiency increases with increasing inhibitor concentration. The inhibitor adsorption on the steel surface follows a Langmuir adsorption indicating a monolayer adsorption. This study confirmed the use of ECE in HCl 1 M solution like a green inhibitor.

Graphical Abstract:

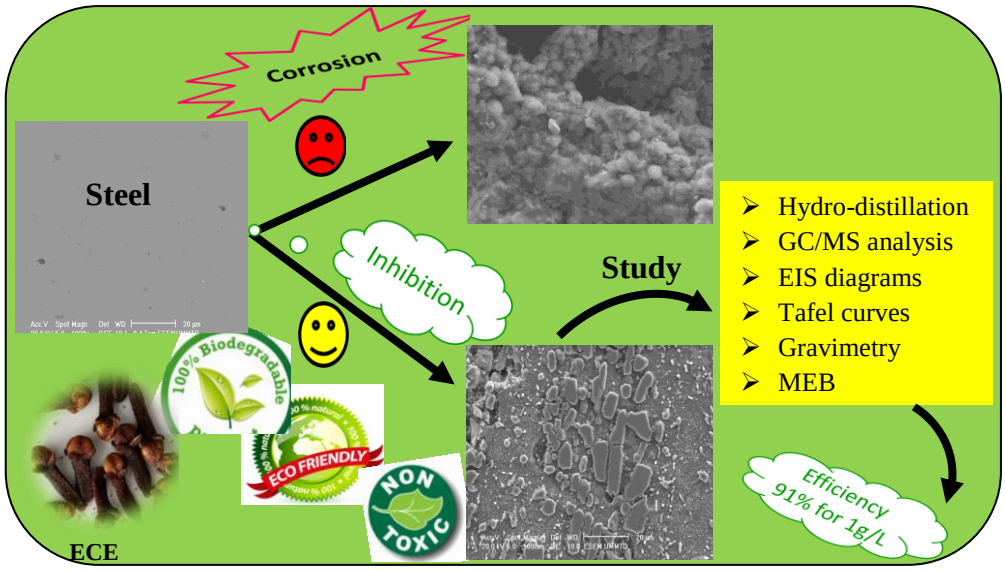

Keywords : *Green inhibitor, corrosion, steel, EIS, Acid, gravimetric, polarization, GC/MS.*

Corresponding author:
Research field: Electrochemistry and Corrosion
Adress : BP 70 B 15000 RP Tizi-Ouzou
E-mail : allamlamia@ummto.dz
Phone : +213.555.713.730
ORCID : 0000-0002-3195-1410

I.Introduction

Carbon steel is extensively used in different industrial applications, such us treatment with acid, alkaline or salt solutions. Those compounds cause severe corrosion and damage to engineering structures. Hence, a protection

by corrosion inhibitors is necessary. Several chemical compounds, which have in their structure N, S, O, P hetero-atoms [1,2], p-electron in triple or conjugated double bonds and aromatic rings [3,4], have been used as corrosion inhibitors of metals.
The current environment requirements imposed eco-friendly (green) corrosion inhibitors, to ovoid the toxicity of synthetic inhibitors. For the purpose, various plant extracts have been found to have anticorrosion effects, in addition to their biological activities. Extract inhibitors from plants, is a cheap and renewable source, then it gained much attention. Consequently, several studies have been intensified on the use of plant extracts and several organic molecules from plants as a green corrosion inhibitor [5-10].

This research reports that the extract of the different parts of the plant (roots, seeds, leaves, stems, flowers and fruits) can be used as corrosion inhibitor of various materials in acid medium [11- 27].

A medicinal plant belonging to the family Myrtaceae has caught our attention; it is the Eugénia Caryophyllata [28]. Its leaves are useful in the preparation of artificial vanillin [29], its flowers and branches are used in pharmacy for medicines in medicine, cosmetic surgery, perfumery and soap factury.

The aim of this work is to study the ECE corrosion inhibition efficiency on carbon steel in 1 M HCl. The extracted molecules, obtained by hydro-distillation of the aromatic dried flowers, was identified by GC-MS. Weight loss and electrochemical tests (potentiodynamic polarization and EIS), were applied. The efficiency was confirmed by SEM.

II.Materials and Methods

II.1. Extraction and characterization of ECE

The Eugenia Caryophyllata flowers were cleaned with distilled water and then dried in the open air and in the laboratory oven at 30°C for 24 hours before being crushed into powder form. The powder was extracted for 3 hours by hydro-distillation with extraction efficiency of 2,25 % and a density of the extract of 1,03. ECE was stored at 4°C in a sealed brown glass tube to keep it from air and light [30].

1 µL of ECE diluted in methanol was analyzed by gas chromatography coupled with mass spectroscopy (GC/MS) SHIMADZU brand GC-MS QP 2010 plus.

II.2. Preparation of samples

The material test is A60 carbon steel, commonly used in general mechanical engineering. For electrochemical measurements, cylindrical steel specimen with a surface area of 0.5 cm^2, coated with polymerizable resin, was used. Rectangular samples with size 2.4 × 1.5 × 0.6 cm, were used for weight loss measurements. Before any test, the samples were mechanically polished on silicon carbide abrasive disks with decreasing roughness (180, 400, 800, 1000, 2000 and 4000) under water jet, followed by polishing on felt by different suspensions (9, 6, 4,... 0.05 µm) of alumina, Al_2O_3. Finally, the samples are cleaned with ethanol in an ultrasonic bath and then rinsed with distilled water and dried in cold air.

II.3. Electrolytic solutions

The corrosive solution is 1 M HCl aerated at ambient temperature and containing different concentrations of ECE (0.1, 0.5 and 1 g/L), maintained under a moderate stirring of 100 rpm.

II.4. Electrochemistry measurements

The electrochemical tests were carried out in a conventional three electrodes cell with Ag/AgCl as a reference electrode (RE) and a platinium with a surface area 0,5 cm^2 as the auxiliary electrode (Aux). These electrodes are connected to Autolab PG STAT 30 potentiostat-galvanostat, controlled by GPES and FRA program for polarization and impedance, respectively.

The evolution of the open circuit potential (OCP) of the working electrode (WE) was measured during the first hour of immersion. Once the stationary state is reached, the polarization curves or EIS diagrams were plotted.

II.4.1. Measurements of linear polarization resistance (LPR)

LPR measurements were obtained by polarization of WE in the immediate vicinity of the corrosion potential E_{corr} ± 20 mV, with 0,16 mV/s scan rate and after 1 hour of immersion. The polarization resistance, R_p, is detrmined from the slope of the *i-E* polarization curve in the neighborhood of E_{corr} , given by Stern and Geary relation [31] :

$$R_p = \left(\frac{\Delta E}{\Delta i}\right)_{E_{corr}} \quad (1)$$

The inhibition efficiency, η , was calculated from the following equation:

$$\eta = \left(\frac{R_p^{inh} - R_p^0}{R_p^{inh}}\right) \times 100 \quad (2)$$

Where R_p^{inh} and R_p^0 are the polarization resistance in the presence and absence of ECE inhibitor, respectively.

II.4.2. Potentiodynamic polarization (PP)

The potentiodynamique i-E curves were obtained at ± 300 mV from E_{corr} with a scan rate of 1 mV/s after 1 hour of immersion time. The extrapolation of the cathodic and anodic Tafel lines, b_c and b_a intersect at E_{corr} and allows the determination of the corrosion current density, i_{corr}.

The inhibition efficiency, η', was evaluated using the following equation:

$$\eta' = \left(\frac{i_{corr}^0 - i_{corr}^{inh}}{i_{corr}^0}\right) \times 100 \quad (3)$$

Where i_{corr}^{inh} and i_{corr}^0 are the corrosion current density in the presence and absence of ECE inhibitor, respectively.

II.4.3. Electrochemical impedance spectroscopy (EIS)

EIS method gives information on the kinetics process of the WE. EIS measurements were performed by Autolab PG STAT 30 potentiostat-galvanostat by means of FRA program. After 1 hour of immersion at OCP, EIS diagrams were plotted at E_{corr} in a frequency range from 10 KHz to 10 mHz and 10 mV of amplitude.

The FRA software allows the determination of the electrical parameters of the metal/solution interface, R_e the resistance of the electrolyte, R_{tc} the charge transfer resistor and *CPE*, the constant phase element, by simulating the impedance diagrams, using an equivalent electrical circuit (Rundles circuit). In the Rundles equivalent circuit, R_e is in series with R_{tc} which is in parallel with a *CPE*. The *CPE* is used when the semicircle is depressed. It is characterized by a proportionality factor *Q* and the phase shift *n* [32], which enables the calculation of the double layer capacitance, $C_{dc,}$ from the following expression:

$$C_{dc} = [Q_{dc}(R_e^{-1} + R_{tc}^{-1})^{n-1}]^{\frac{1}{n}} \quad (4)$$

Inhibition efficiency, η'' , was calculated replacing R_p^{inh} and R_p^0 by R_{tc}^{inh} and R_{tc}^0 in equation (2), respectively.

II.5. Non-electrochemical measurements

II.5.1. Gravimetric measurements and microscopic surface characterization

The rectangular steel samples (2,4 × 1,5 ×0,6 cm), finely polished and dried as before, were weighed on an analytical balance with 10^{-4} precision and vertically immersed for 7 days in a beaker of 100 mL containing 50 mL of stagnant solution with different concentrations of ECE at room temperature (25 ± 2°C). At the end of the experiment, the freely corroded and inhibited samples were rinsed with distilled water followed by degreasing in acetone under ultrasound and dried under air flow before being weighed.

The weight loss ΔW was determined from the sample mass difference, ($m_0 - m$) before and after immersion in the corrosive medium at different concentration of ECE. The corrosion rate, V_{corr} , in $mg.cm^{-2}.h^{-1}$ was calculated from the following relation:

$$V_{corr} = \frac{\Delta W}{S \times t} \quad (5)$$

Where, S: submerged sample surface, t: immersion time.

The inhibition efficiency, η''', was evaluated from the corrosion rate as following:

$$\eta''' = \frac{V_0 - V_{inh}}{V_0} \times 100 \quad (6)$$

Where, V_0 and V_{inh} represent corrosion rate of steel, in the absence and presence of inhibitor, respectively.

The surface coverage, θ, was calculated from the inhibition efficiency :

$$\theta = \frac{\eta}{100} \quad (7)$$

The morphology of the steel surface was performed on the samples immersed in HCl without and with ECE for 7 days, using PHILIPS ESEM XL 30 scanning electron microscope.

II.6. Adsorption isotherms

Adsorption isotherms indicate the interaction between the metal and the inhibitor and its adsorption mechanism. In generally, it is a substitution process of water molecules by inhibitor molecules. [33]
Various models of adsorption process of ECE on the steel surface were proposed: Langmuir, Frumkin and Temkin, which were represented by the following equations:

Isotherm of Langmuir :

$$\frac{C_{inh}}{\theta} = \frac{1}{K_{ads}} + C_{inh} \quad (8)$$

Isotherm of Temkin :

$$e^{-2a\theta} = K_{ads} C_{inh} \quad (9)$$

Isotherm of Frumkin :

$$\frac{\theta}{1-\theta} e^{-2\theta} = K_{ads} C_{inh} \quad (10)$$

Where, θ : the coverage rate of the inhibitor molecules on the steel surface, calculated from the equation (7), a : the constant of the heterogeneity of the surface and intermolecular interactions of the adsorbed inhibitor film, K_{ads} : the equilibrium constant of the adsorption process.

III.Results and discussions

III.1. Characterization GC/MS

We propose hereafter the experimental results of two protocols obtained by GC/MS where interest resides in the interpretation of the spectra. At the end of the GC, the chromatogram detects the molecule corresponding to this chromatogram. Once the SM analysis is completed, the software compares the *m/z* ratios over the entire experimental interval with its tandem in the database (theoretical) with an identification percentage of 99%. The analysis protocol gave the following chromatogram:

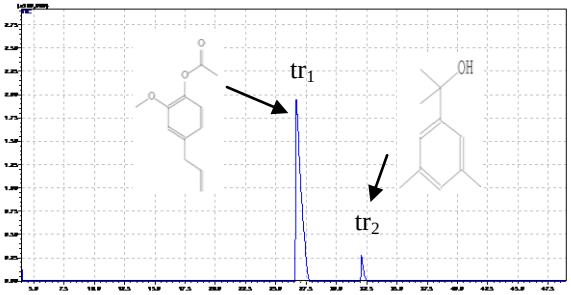

Fig. 1: Chromatogram of the ECE.

Fig.1. illustrates, on the one hand, the molecule corresponding to tr_2 = 22,5 is a derivative product due to the rearrangement of the acetate eugenol following the electron bombardment on the latter. It should be noted that the presence ratio of the second peak relative to the first peak is 12.5%. It is probable that the formation of this derivative is due to the injection protocol and to the temperature gradient used in the experiment; it can then be excluded from the interpretation.

The mass spectrum obtained corresponding to the peak 1at tr_1 = 27,5 is the following.

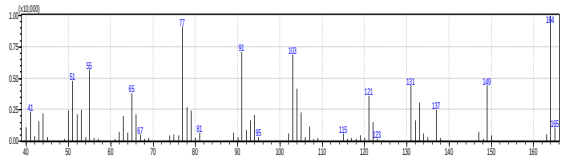

Fig. 2: Experimental mass spectrum for peak1

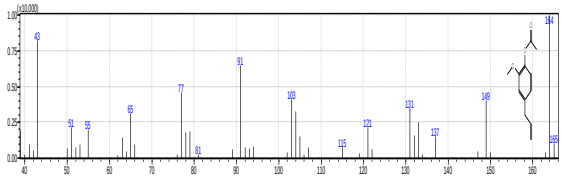

Fig. 3: Theoretical mass spectrum of eugenol-acetate

The superposition of this experimental spectrum with the different base spectra of Data revealed a single spectrum identical to the experimental obtained at 99% which is that of the eugenol acetate shown schematically in Fig. 4.

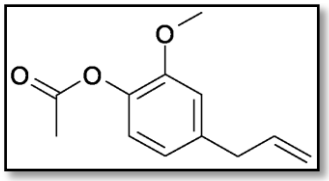

Fig.4: Chemical structure of ECE inhibitor

III.2. Electrochemistry measurements

III.2.1. Open circuit potential (OCP)

The shape of the E-t curve gives information about the phenomena that occurs at the metal/solution interface, which makes it possible to determinate stationary system. Without inhibitor, the potential decreases and becomes less and less noble, to stabilize at -0.69 V/Ag-AgCl, after 20 hours of immersion. There is therefore a continuous and local attack of the steel by the H^+ and Cl^- ions of the solution which cause the potential fluctuations and shifting towards more electronegative values. With ECE addition, E_{corr} shifts towards nobler potentials; this indicates the benefits increase of the inhibitor with increasing ECE concentration.

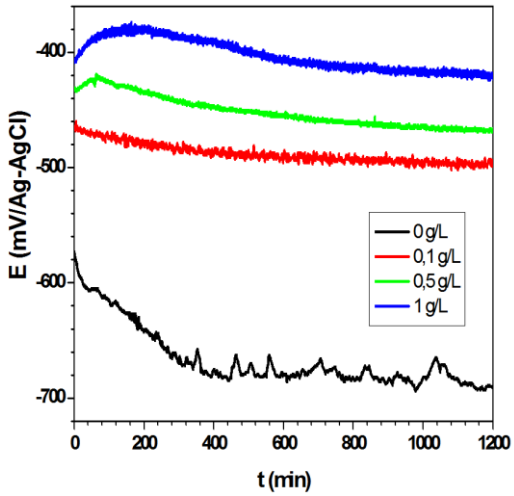

Fig.5: OCP of steel in the absence and presence of ECE.

III.2.2. Polarization resistance measurements

The R_p values obtained from LPR were listed in Table I. We note that increase in ECE concentration, C_{ECE}, induced an increase in R_p values, which suggests the formation of a protective nonconductive film, adsorbed on the steel surface.

Table I : LPR data of steel in 1 M HCl without and with ECE.

C_{ECE} (g/L)	LPR	
	R_p ($\Omega.cm^2$)	η (%)
0	0.0357	-
0.1	0.1009	64.6
0.5	0.13	72.5
1	0.168	79

III.2.3. Potentiodynamic polarization measurements

Fig. 4 shows the global polarization curves of carbon steel after 1 hour of immersion in 1 M HCl with different ECE inhibitor concentration. The same general shape of the curves is obtained, where two domains were observed:

Cathodic field described by the following reaction :

$$2H^+ + 2e^- \rightarrow H_2 \qquad (11)$$

Anodic field of steel dissolution with a passivation plateau according to the following reaction:

$$Fe \rightarrow Fe^{2+} + 2e^{-} \qquad (12)$$

When the concentration of the inhibitor increases, a decrease of the anodic and cathodic current densities is observed. This result indicates that ECE is a mixed inhibitor, which is in agreement with the work of Den et *al*. [34], Kina et *al*. [35] and Vra et *al*. [36].

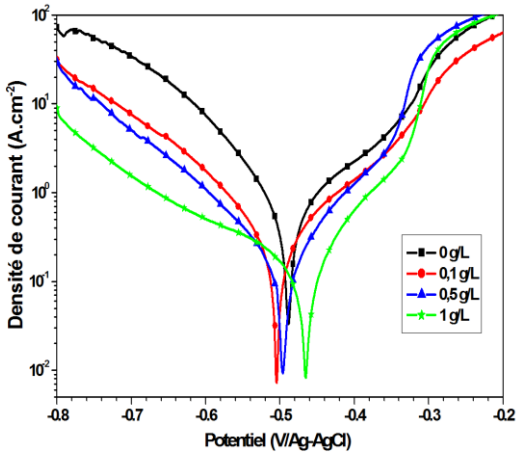

Fig. 6: Polarization curves of steel in the presence and absence of ECE.

The cathodic and anodic Tafel lines were obtained graphically. The corrosion current density was obtained by extrapolating the linear portions of Tafel curves to the intersection at E_{corr}, based on the cathodic line because the anodic Tafel slopes were not determined in the Tafel domain due to the presence of a passivation plateau.

The following table regroups the electrokinetic parameters values determined graphically from the straight lines of Tafel curves.

Table II: Values of electrokinetic parameters obtained from polarization curves

C_{ECE} (g/L)	E_{corr} (V/AgCl)	b_a (V/dec)	$-b_c$ (V/dec)	i_{corr} (mA.cm^{-2})	η' (%)
0	-0.487	-	0.130	1.333	-
0.1	-0.504	0.150	0.147	0.320	75.99
0.5	-0.497	0.122	0.170	0.222	83.35
1	-0.460	0.107	0.215	0.119	91.07

The following observations can be made:

- The addition of the inhibitor varied slightly the values of the cathodic Tafel slopes b_c., which suggests that proton reduction mechanism is partially unaffected by the addition of the inhibitor.

- The i_{corr} values decrease with the increase of the ECE concentration compared to blank test, this is due to the blocking effect of the active sites on the metal surface by the adsorbed inhibitor molecules [37].

- The calculated values of η' increase with the concentration to reach a maximum of 91% at 1 g/L. This excellent efficiency is explained by the presence of the high electronic densities on the inhibitor molecules due to the existence of the non-binding doublets of the oxygen and the π electrons of the aromatic nucleus, which favors the adsorption process on the steel [38-39]. This last can occur directly by acceptor-donor interactions between the free doublets and the π electrons of the inhibitor molecule with the *d* orbitals of the metal [1].

III.2.4. Impedance measurements

The experimental and adjusted impedance diagrams are shown in Fig. 7, in Nyquist mode. An enlargement of the spectra is proposed in order to discern the high frequencies domain of the diagrams.

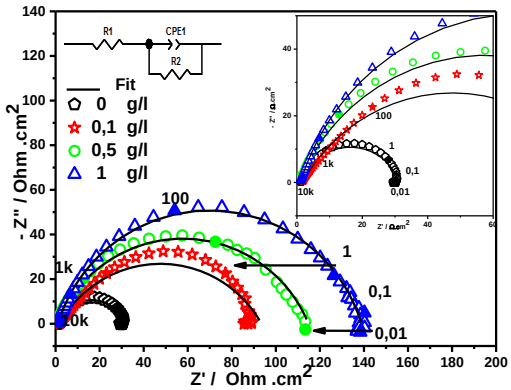

Fig. 7: Nyquist plots of impedance diagrams of steel after 1 hour immersion in 1 M HCl with and without ECE.

These diagrams show a capacitive behavior of the interface over the entire frequency domain,

represented by a single loop with a diameter equivalent to the charge transfer resistance, R_{tc} [40] and its value increases with increasing inhibitor concentration.

It appears that those loops are not perfect semi-circles, which means it's not centered on the real axis. This can be attributed to the frequency dispersion due to the heterogeneity of the electrode surface [41-42], hence the necessity of the constant phase element (CPE) which accounts for its heterogeneities, through the coefficient *n*. According to some authors [28-29], this non-perfect capacitive loop results from roughness, impurities, adsorption of the inhibitor and/or formation of porous layers, which generally indicates that the reaction of corrosion is controlled by a charge transfer process on heterogeneous and irregular solid surface electrode [43-44].

Indeed, during the process of immersing the steel in the solution, the molecules of the inhibitor adsorb on the electrode surface. Thus, the formed film serves as a blocking barrier which would prevent the corroding ions of the electrolyte from reaching the surface of the electrode, which effectively protect it against corrosion.

A better 3-D visualization for the Nyquist diagram is shown in Fig. 8.

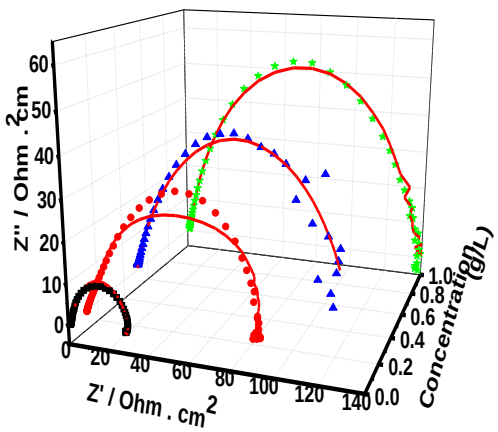

Fig. 8: A better 3-D visualization for the Nyquist diagram is shown in figure

The equivalent electrical circuit represented in the insert gave excellent spectral adjustment with good correlation (< 0.01). The electrical parameters (R_e, R_{tc} and *CPE*) of the equivalent circuit and the inhibitory efficiency, obtained from the impedance diagrams are summarized in Table III.

Table III. Values of electrical parameters obtained from Nyquist impedance diagrams

C_{inh} (g/L)	R_e ($\Omega.cm^2$)	R_{tc} ($\Omega.cm^2$)	CPE		C_{dc} ($\mu F.cm^{-2}$)	$\eta_{,,}$ (%)
			$Q.10^3$ ($\Omega^{-1}.cm^{-2}.s^n$)	n		
0	1.05	30	2.3	0.78	416	-
0.1	1.78	91.7	1.35	0.67	65.1	67.28
0.5	0.625	114.2	0.265	0.75	14.5	73.73
1	1.05	137.8	0.316	0.81	48.2	78.23

Fig. 9 shows the evolution of the inhibition efficiency with different concentrations of ECE, and as expected the efficiency increases with the ECE concentration. The values obtained with the different measurement techniques are in good agreement and have shown that ECE can serve as an effective inhibitor against corrosion.

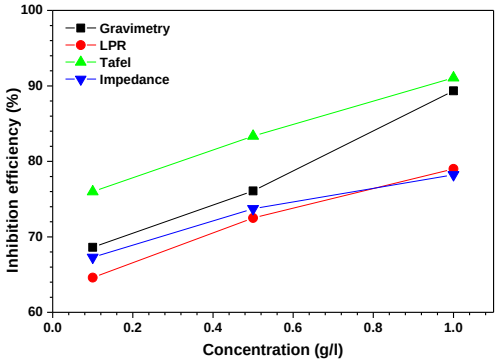

Fig. 9: Inhibition efficiency of ECE on steel corrosion in 1 M HCl.

III.3. Non-electrochemical measurements

III.3.1. Gravimetric measurements and microscopic surface characterization

Gravimetric tracking of η''' and ΔW is carried out for reasons of simplicity of the process and corrosion data approaches service conditions more accurately, hence its use by several

researchers [19]. Table IV summarizes the values of V_{corr} and η''' obtained by gravimetry at different concentrations of ECE in 1 M HCl, after 7 days of immersion of steel.

Table IV: Gravimetric data obtained after 7 days of immersion of steel in HCl 1M with and without ECE.

C_{EEC} (g/l)	Gravimetry			
	ΔW (g)	V (mg.cm^{-2}.h^{-1})	η'''(%)	θ
0	2.386	1.351	-	-
0.1	0.723	0.424	68.62	0.69
0.5	0.550	0.323	76.09	0.76
1	0.246	0.144	89.34	0.89

We note from Table IV, that the inhibition efficiency increases with increasing inhibitor concentration to a maximum value of 89.34% for 1 g/L of ECE, following a decrease in corrosion rate. This suggests that ECE is increasingly adsorbed on the steel surface and covers the active sites.

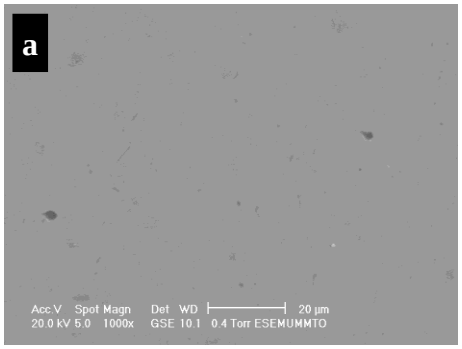

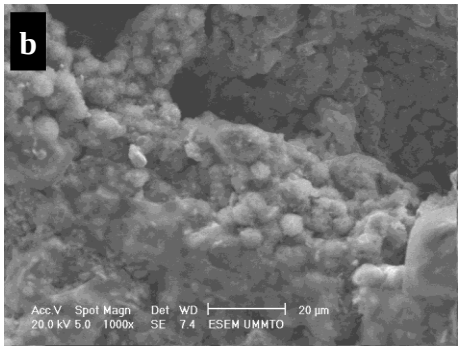

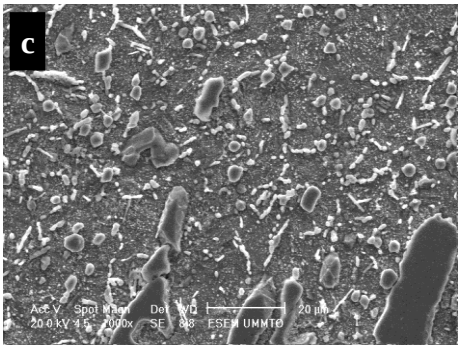

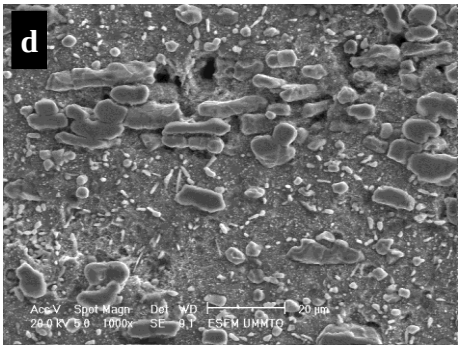

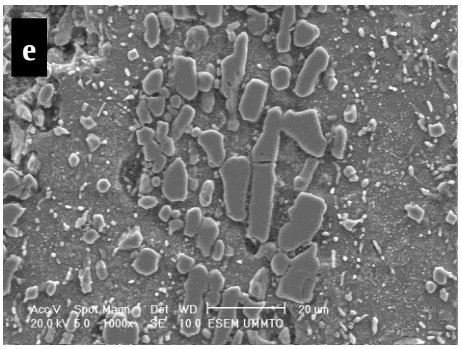

Fig. 10 : SEM images of steel (a) before and after 7 days of immersion in (b) 1 M HCl, (c) 1 M HCl + 0.1 g/L ECE, (d) 1 M HCl + 0.5 g/L ECE, e) 1 M HCl + 1 g/L ECE

The SEM images shown in Fig. 10 confirm the results of the electrochemical measurements. Severe corrosion of the entire steel surface immersed in 1 M HCl is observed (image b) and compared to the polished steel prior to immersion (image a), where a smooth and homogeneous surface is seen. On the other hand, Figures. 10c. , 10d. and 10e, reveal the surface state of the protected samples, by the addition of different concentrations of the ECE inhibitor. This is due to the formation of an adsorbed layer on the steel surface. These observations show that the extract prevents steel

corrosion by limiting access to the acid on the surface, which increases its resistance to corrosion. The three images show that ECE molecules cover more area with increasing inhibitor concentration. At low concentration, low surface coverage, consequently, large attacked surface.

III.4. Adsorption isotherms

Fig. 11. represents the set of isotherms obtained for the ECE inhibitor. For each representation, the linear regression was plotted from calculated experimental data. The analysis of these curves shows that, the variation of the ratio $\frac{C_{inh}}{\theta}$ as a function of C_{inh} is linear and fit well the experimental data.

This indicates that the adsorption of the inhibitor molecules on the steel surface obeys the Langmuir adsorption isotherm. The model was reported by Faustin [45] and Suedile [46] and it was in generally considered to represent adsorption phenomena involved in corrosion inhibition processes, due to the formation of monolayer coverage on the adsorbent surface, limiting the access of the electrolyte. Langmuir adsorption assumes that the solid surface contains a determined number of adsorption sites and that each site can accommodate only one adsorbed species. Moreover, the adsorbed molecules do not interact with each other and all adsorption sites are thermodynamically equivalent [45-46].

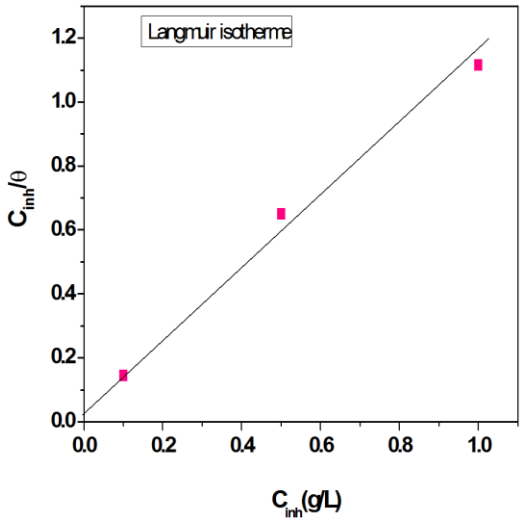

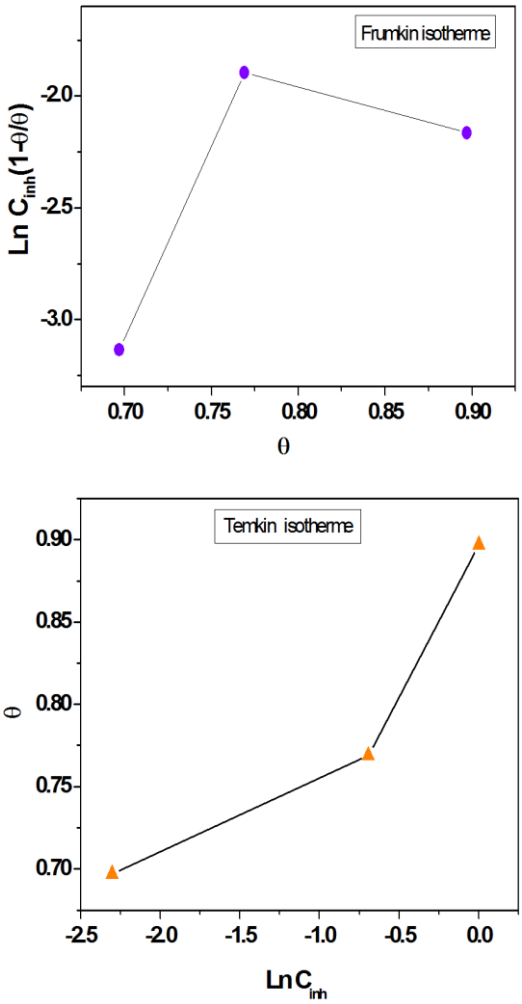

Fig. 11 : Langmuir, Frumkin and Temkin adsorption isotherms for steel in 1 M HCl in the presence of ECE at 25°C

IV. Conclusions

The gravimetric method has shown that the corrosion rate decreases while the efficiency increases to reaches a maximum value at a concentration of 1 g/L of ECE. The electrochemical method revealed that the addition of ECE inhibitor at increasingly concentrations led to decrease the current densities of both cathodic and anodic branches with a slight displacement of the corrosion potential on both sides, which indicates a mixed character of the ECE inhibitor. The EIS method gave a significant increase in the charge transfer resistance as the concentration of ECE

increases, which justify the adsorption of this inhibitor on the steel surface. SEM observations confirmed the presence of a protective layer formed on the metallic surface in the presence of the extract. Moreover, the plot of the different adsorption isotherms (Langmuir, Temkin and Frumkin), showed that the adsorption of ECE is well fitted to the Langmuir adsorption model. This model assumes that the adsorption is monomolecular and that the interactions between absorbed particles are negligible.

All results, via electrochemical and non-electrochemical methods, are in good agreement and show a highest inhibition efficiency at 1 g/L of ECE inhibitor, which confirm that ECE can be used as corrosion inhibitor for steel in 1M HCl bath.

References

[1] 26 H. Zarrok, H. Oudda, A. Zarrouk, R. Salghi, B. Hammouti, M Bouachrine, *Der Pharma Chemica., 3 (2011) 576.*

[2] B. Hammouti, R. Salghi, S. Kertit, *J. Electrochem. Soc. India, 47 (1998) 31.*

[3] Ouchrif, A. Yahi, B. Hammouti, A. Dafali, M. Benkaddour, E. Touhami, *Bull. Electrochem., 19 (2003) 445]*

[4] V.B. Dhayabaran, A. Rajendran, J.R. Vimala, A. Anandhakumar, Tans. *SAEST, 40 (2005) 134.*

[5] K.W Tan and M.J Kassim, *Corros.Sci., 52 (2011) 569.*

[6] G. Blustein, A.R.D. Sarli, J.A Jaen, R.Romagnoli and B.D. Amo, *Corros. Sci., 49 (2007) 4202.*

[7] M. Salasi, T. Saharabi, E. Rooyali and M. Ali of KHAZRAEI, *Mater. chem. phys., 104 (2007) 183.*

[8] G. Gunasekaran, L.R. Chauhan, *Eco friendly inhibitor for corrosion inhibition of mild steel in phosphoric acid medium, Electrochim. Acta, 49 (2004) 4387-4395.*

[9] A. Y. El-Etre, M. Abdellah, Z.E. El-Tantawy, *Corrosion inhibition of some metals using lawsonia extract, Corros. Sci., 47 (2005) 385-395.*

[10] L.R. Chauhan, G. Gunasekaran, *Corrosion inhibition of mild steel by plant extract in dilute HCl medium, Corros. Sci., 49 (2007) 1143-1161.*

[11] M. Faustin, M. Lebrini, F. Robert, and C. Roos, "*Corrosion studies of C38 steel by Alkaloids extract of a tropical plant type," International Journal of Electrochemical Science, 6 (9) (2011) 4095-4113.*

[12] M. Salasi, T. Saharabi, E. Rooyali and M. Ali of KHAZRAEI, *Mater. chem. phys.,104 (2007) 183.*

[13] M. Benabdellah, M. Benkadour, B. Hammouti, M. Bendahhou, A. Aouniti, *Inhibition of steel corrosion in 2M H3PO4 by Artemisia oil, Appl. Sur. Sci. 252 (2006) 6212-6217*

[14] P.C. Okafor, M.E. Ikpi, I.E. Ebenso, U.J. Ekpe, S.A. Umoren, *Inhibitory action of Phyllanthus amarus extracts on the corrosion of mild steel in acidic media, Corros. Sci., 50 (2008) 2310-2317.*

[15] A. Ostovari, S.M. Hoseinieh, M. Peikari, S.R. Shadizadeh, S.J. Hashemi, *Corrosion inhibition of mild steel in 1M HCl solution by henna extract: A comparative study of the inhibition by henna and its constituents (Lawsone, Gallic acid, α-D-Glucose and Tannic acid), Corros. Sci., 51 (2009) 1935-1949.*

[16] A.K. Satapathy, G. Gunasekaran, S.C. Sahoo, Kumar Amit, P.V. Rodrigues, *Corrosion inhibition by Justicia gendarussa plant extract in hydrochloric acid solution, Corros. Sci., 51 (2009) 2848-2856*

[17] S. Garai, S. Garai, P. Jaisankar, J.K. Singh, A. Elango, *A comprehensive study on crude methanolic extract of Artemisia pallens (Asteraceae) and its active component as effective corrosion inhibitors of mild steel in acid solution, Corros. Sci., 60 (2012) 193-204.*

[18] X. Li, S. Deng, *Inhibition effect of Dendrocalamus brandisii leaves extract on aluminum in HCl, H3PO4 solutions, Corros. Sci. 65 (2012) 299-308.*

[19] X. Li, S. Deng, *Inhibition effect of Dendrocalamus brandisii leaves extract on aluminum in HCl, H3PO4 solutions, Corros. Sci., 65 (2012) 299-308.*

[20] N. Soltani, N. Tavakkoli, M. Khayat Kashani, M. R. Jalali, *Green approach to corrosion inhibition of 304 stainless steel in hydrochloric acid solution by the extract of Salvia officinalis leaves, Corros. Sci., 62 (2012) 122-135.*

[21] A.F. Gualdron, E. N. Becerra, D. Y. Pena, J. C. Gutiérrez, H. Q. Becerra, *Inhibitory effect of Eucalyptus and Lippia essential oils on the corrosion of mild steel in hydrochloric acid, J. Mater. Environ. Sci., 4 (2013) 143-158.*

[22] D. Benmessaoud Left, M. Zertoubi, A. Irhzo, M. Azzi, *Review: Oils and extracts plants as inhibitors for different metals and alloys in hydrochloric acid medium, J. Mater. Environ. Sci., 4 (2013) 855-866.*

[23] M. Chevalier, F. Robert, N. Amusant, M. Traisnel, C. Roos, M. Lebrini, *Enhanced corrosion resistance of mild steel in 1M hydrochloric acid solution by alkaloids extract from Aniba rosaeodora plant: Electrochemical, phytochemical and XPS studies, Electrochim. Acta, 131 (2014) 96-105.*

[24] X. Li, S. Deng, X. XIE, H. Fu, *Inhibition effect of bamboo leaves' extract on steel and zinc in citric acid, Corros. Sci., 87 (2014) 15-26.*

[25] H. Bentrah, Y. Rahali, A. Chala, Gum Arabic as an eco-friendly inhibitor for API 5L X42 pipeline steel in HCl medium, *Corros. Sci., 82 (2014) 426-431.*

[26] N. Soltani, N. Tavakkoli, M. Khayat Kashani, A. Mosavizadeh, E.E. Oguzie, M.R. Jalali, *Silybum marianum extract as a natural source inhibitor*

for 304 stainless steel corrosion in 1M HCl, J. Indus. Engin. Chem., 20 (2014) 3217-3227.

[27] M. Faustin, A. Maciuk, P. Salvin, C. Roos, M. Lebrini, Corrosion inhibition of C38 steel by alkaloids extract of Geissospermum laeve in 1M hydrochloric acid: Electrochemical and phytochemical studies, *Corros. Sci., 92 (2015) 287-300.*

[28] Speck. Brigitte, *Ursula. &Fotsch Christian, Connaissance des herbes, EGK-CAISSE de santé, (2011).* www.egk.ch

[29] J. Minelle, l'Agriculture à Madagascar, *Eds. Librairie Marcel Riviére et cie, (1959) 3-6.*

[30] S. Burt, Essential Oils, their antibacterial properties and potential applications in foods – arevieo, International journal of food Microbiology 94, (2004) 223-253.

[31] M. Stern, A.L. Geary, *J. Electrochem. Soc., 104 (1957) 56.*

[32] M. Hukovic-Metikos, R. Babic, Z. Gutac, *J. Appl. Electrochem., 32 (2002) 35.*

[33] F. Zulkifli, Nora'aini Ali, M. Sukeri M. Yusof, Wan M. Khairul, Fafizah Rahamathullah, M.I.N. Isa, W. B. Wan Nik, *Advances in Physical Chemistry, (2017) 12 pages. https://doi.org/10.1155/2017/8521623*

[34] X .U. Li, S.D. Deng, Corros. Sci., 509 (2008) 420.

[35] L. Kinani, A. Chtaini, H. Latrache, "The Inhibition Effect of Eugenol to the Biocorrosion of Titanium in Saliva Medium," *24 (2014) 51-59. ISSN 1583-1078.*

[36] L.J.M. Vračar, D.M. DRAZIC, *Corros. Sci., 44 (2002) 1669.*

[37] X. Li, "Inhibition effect of 6 – benyylaminopurine on the corrosion of cold rolled steel in H_2SO_4 Solution," Corros. Sci., 51 (2009) 620 – 634.

[38] A. H. Mehaute, G. Gepy, Solid state Ionics, 17 (1989) 910.

[39] G. Reinhard, U. Rammet, *6thEuropean Symposium on Corrosion Inhibitors*, Ann. (Univ. Ferrara, Italy, *1985)* 831.

[40] K.F. Khaled, N. Hackerman, *Mater. Chem. Phys., 82, (2003) 949.*

[41] M. Lebrini, M. Legrenee, H. Vezin, M.Traisnel, F. Bentiss, "Experimental and theoretical study for corrosion inhibition of mild steel in normal hydrochloric acid solution by some new macrocyclic poly ether compounds," *Corros. sci., 49 (2007) 2254 - 2269.*

[42] F. Mansfeld, M.W Kending, S .Tsai, *Corrosion 37 (1982) 301.*

[43] M. Duprat, F. Dabosi, F. Moran, Rochers, "Inhibition of corrosion of a carbon steel by the aliphatic fatty polyamines in association with organic phosphorous compounds in 3% sodium chloride solution," *Corrosion -Nace, .37 (1981) 262-266.*

[44] A. Popova, S. Raicheva, E. Sokolova, Langmuir, 12 (1996) 2083.

[45] M. Faustin, "Etude de l'effet des alcaloïdes sur la corrosion de l'acier C38 en milieu acide chlorhydrique 1M : Application à Aspidosperma Album et Geissopermumlaexe (Apocynacées)," Thèse de Doctorat (Université des Antilles et de la Guyane 2013).

[46] F. Suedile, "Extraction, Caractérisation et études électrochimique de molécules actives issues de laforet amazonienne pour la protection du zinc contre la corrosion," Thèse de Doctorat (Université des Antilles et de la Guyane 2014).